Acta Biomed 2015; Vol. 86, N. 1: 77-85

Original article

Coronary CT angiography using iterative reconstruction vs. filtered back projection: evaluation of image quality

Teresa Arcadi[1], Erica Maffei[2], Cesare Mantini[3], Andrea I. Guaricci[4], Ludovico La Grutta[5], Chiara Martini[2], Filippo Cademartiri[2]

[1] Department of Radiology, SDN IRCCS, Naples, Italy; [2] Cardiovascular Imaging Unit, Department of Radiology, Giovanni XXIII Clinic, Monastier di Treviso, Treviso, Italy; [3] Department of Radiology, University of Chieti, Italy; [4] Department of Cardiology, University of Foggia, Italy; [5] Department of Radiology, University of Palermo, Italy; [6] Department of Radiology, Erasmus Medical Center University, Rotterdam, The Netherlands

Summary. *Objectives:* To compare image quality of iterative reconstruction algorithm(IRIS) vs. standard filtered back projection(FBP) reconstruction in CT Coronary Angiography (CTCA). *Materials and methods:* Thirty-four consecutive patients underwent CTCA for suspected or known CAD with Dual-Source CT (DSCT-Flash, Siemens). All datasets were reconstructed with 0.75/0.4 and 0.6/0.4 mm slice thickness/increment, using three standard FBP kernels (B26-B30-B46) and three comparable IRIS algorithms (I26-I30-I46). Vascular attenuation and noise were measured. CT vascular attenuation values [HU] were measured in: ascending aorta (Ao), right (RCA) and left (LCA) coronary artery, respectively. Signal-to-noise (SNR) and contrast-to-noise (CNR) ratio were calculated. A p-value<0.05 was considered significant. *Results:* There was no significant difference between the vascular attenuation values measured with FBP (Ao:458HU, RCA:448HU, LAD:444HU) and IRIS (Ao:456HU, RCA:446HU, LAD:442HU). Difference in noise was significant between FBP (24±SD) and IRIS (19±SD) (r=0.34;p<0.05). Lowest noise was found for IRIS using 0.6 mm (17HU). IRIS provided a SNR and CNR significantly higher with increasing kernel sharpness. SNR was 33.3±25.1, 77.3±51.7, 37.2±36.6, 64.4±59.2, while CNR was 25.32±19.8, 58.0±36.0, 28.6±23.5, 47.6±47.3 for 0.75B, 0.75I, 0.6B and 0.6I, respectively. IRIS showed an improvement in SNR of 57% and 56% for 0.75 mm and 0.6 mm, respectively, and an improvement in CNR of 42% and 40% for 0.75 mm and 0.6 mm. *Conclusions:* In CTCA, iterative reconstructions provide a significant higher image quality compared with the conventional FBP reconstructions. (www.actabiomedica.it)

Key words: iterative reconstruction, signal, noise, cardiac CT, filtered back projection

Introduction

Computed tomography coronary angiography (CTCA) has a high sensitivity and high negative predictive value (NPV) for detecting significant coronary stenoses (i.e. lumen diameter reduced by ≥50%) in patients with suspected coronary artery disease (CAD), when compared with invasive coronary angiography (1- 5).

CTCA does not only provide information about luminal narrowing of the coronary artery tree but also allows the noninvasive detection of coronary atherosclerotic plaque (6). CTCA can detect coronary artery calcium and noncalcified components of the coronary artery atherosclerotic plaque. CTCA can be used to assess some characteristics of the "vulnerability" of plaques, such as positive remodeling, eccentricity and

noncalcified components, which are associated with a higher risk of cardiovascular events (6).

However, the ability to detect and distinguish the different types of plaque with CT is still under investigation (7). Although CTCA has been shown to be highly accurate in detection of calcified plaque, various studies have demonstrated limitations in detection of noncalcified plaque (8, 9) due to the limited contrast resolution influenced by the noise of the CT images (6). Thereby, qualitative and quantitative imaging parameters to characterize plaque at CT may be helpful to improve risk stratification in patients with CAD (10).

CT coronary atherosclerosis assessment is based on the variable X-ray attenuation of the tissue components and several parameters, such as lumen attenuation, body mass index, convolution filtering, and contrast-to-noise ratio (CNR) are able to influence the attenuation values used to define the composition of coronary plaque (11-26).

Traditional limitation of Cardiac CT are related to image noise, blooming artifacts from calcification and stents, and radiation exposure.

Recently, a number of alternative image CT reconstruction techniques have been used with the goal to preserve or improve image quality and/or reduce radiation dose, such as iterative reconstruction (IR). One of the first IR algorithms released for clinical use was the iterative reconstruction in image space (IRIS) algorithm (Siemens Medical Solution, Foreign, Germany).

The filtered back projection (FBP), the so-called analytic reconstruction techniques, is currently the gold standard on all modern CT systems. Analytic reconstruction algorithms such as FBP rely on the exact mathematical relationship between the measured x-ray-attenuation in the projection data and the pixel values in the corresponding image, producing an exact image. Nevertheless, the exact projection data from the scanner are noisy, so this noise is amplified by the filter of FBP.

Unlike FBP, IRIS reduces image noise by forming iterations between raw data and image space, generating images of higher image quality than FBP in the setting of a very low SNR (27-29). IRIS technique uses a statistical model of the noise enables to selectively identify image noise by taking into account fluctuations in projection measurement due photon statistics and electronic noise statistics (quantum noise). IRIS entails fewer assumptions regarding noise distribution within an image and operates with an iterative process of mathematic and statistical modeling to identify and selectively reduce noise (30-32), and unlike advanced iterative reconstruction is computationally less demanding.

We hypothesized that IRIS is superior to FBP reconstructions in the signal detection and contrast resolution. Therefore, the purpose of this study was to compare image quality of IRIS vs. FBP in CTCA.

Materials and methods

Study population

Between October 2010 and August 2011 we prospectively enrolled 34 patients (20 men, 14 women; age = 60.3±13.2 years) who were referred for CTCA for coronary artery evaluation. Patients in sinus heart rhythm who were able to hold their breath for 12s and without contraindications to the iodinated contrast agents administration (e.g., known allergy, kidney failure or thyroid disorders) were included.

Demographic and clinical signs and symptoms details of the enrolled subjects as well as associated cardiovascular risk factors are summarized in Table 1. Informed consent was obtained from all patients and the local Medical Ethical Committee approved the study.

Patient preparation

Upon arrival, blood pressure and heart rate (HR) were measured and 5-20 mg of intra-venous atenolol (Tenormin, AstraZeneca) were administered if the HR exceeded 65 bpm, in order to reach an HR below 65 bpm. Just before the CT data acquisition 0.3 mg of sublingual nitroglycerin (isosorbide dinitrate, Carvasin 5 mg, Wyeth Lederle) was administered in the absence of contraindications.

CT scan protocol

The study was performed with a 128-slice dual-source CT (DSCT) scanner (Somatom Definition Flash; Siemens, Forchheim, Germany) (33, 34). All

Table 1. Study population

	Total
Population	
Number of patients	34
Age (years; mean±SD) 61.2±11.6	60.3±13.2
Gender (M/F)	20/14
BMI (mean±SD)	28.86±4.14
Cardiovascular risk factors	
Hypertension	17 (50)
Hypercholesterolaemia	18 (53)
Diabetes	3 (9)
Cigarette smoking	53 (33)
Family history	0 (0)
Obesity (BMI≥30 kg/m2)	9 (27)
Heart rate (bpm; mean±SD)	63.4±17.6
LVEF (%; mean±SD)	52.0±15.7

Abbreviations: SD, standard deviation; M/F, males/females; BMI, body mass index; bpm, beats per minute; LVEF, left ventricle ejection fraction

patients underwent an un-enhanced CT scan for the coronary calcium quantification followed by an angiography scan.

The following parameters were used for the ECG-gated spiral CT coronary angiography: number of slices per rotation 64×2×2; detector collimation: 64×0.6 mm; gantry rotation time 280 ms; effective temporal resolution 75 ms; tube voltage 100-120 kV [according to patient body mass index (BMI)]; tube current 320-370 mAs (according to patient BMI); craniocaudal scan direction; reconstruction algorithm 180°; patient table feed/pitch variable and adapted to HR (range 0.16-0.35). Prospective tube current modulation was used with a high-dose window from 65% to 80% of the RR interval and a MinDose protocol (Siemens, Germany) in the remaining phases of the cardiac cycle (i.e. 4% of maximum amperes; Figure 1). For contrast enhancement, 70-100 mL of contrast medium (Iomeprol, Iomeron 400, Bracco, Milan, Italy) was administered intravenously at 5-6 mL/s (2 g iodine/s) flow rate, followed by 40 mL of saline chaser at same flow rate using an automatic injector (Stellant, MedRAD, Pittsburgh, PA, USA) attached to an 18- to 20-gauge needle cannula positioned in an antecubital vein (33, 34). A bolus tracking technique (CARE bolus, Siemens, Forchheim, Germany) for contrast bolus arrival and data acquisition synchronization was used (33, 35). The anatomical coverage extended from the tracheal bifurcation to the diaphragm. Angiography scan data were obtained during a single breath-hold of 4–7 s (according to HR and adaptive pitch). Retrospective

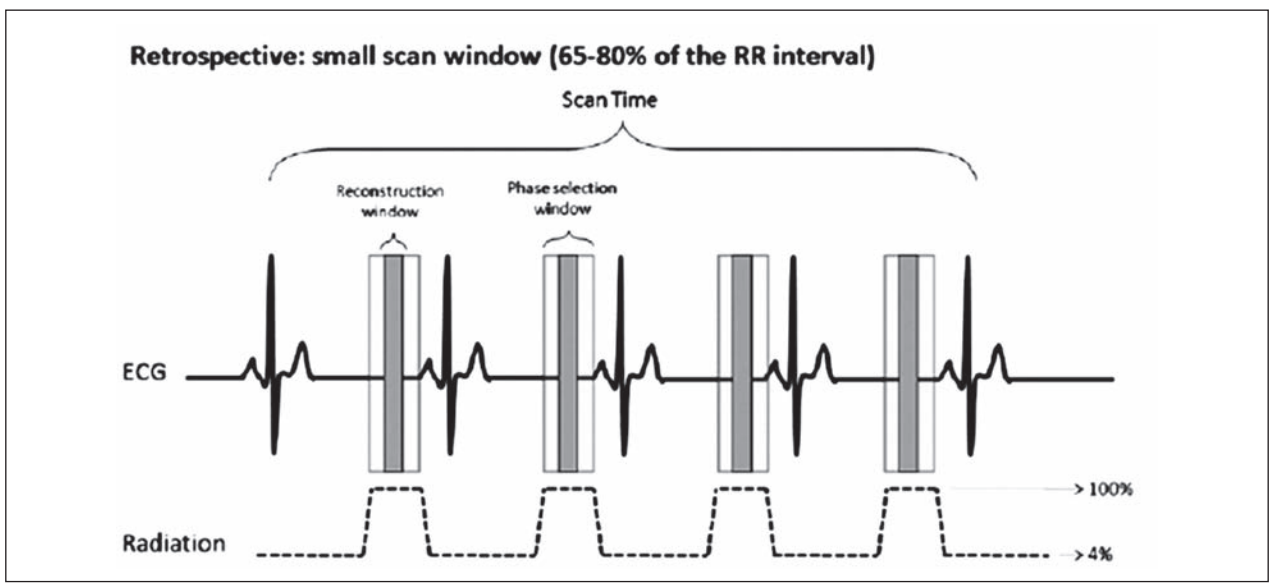

Figure 1. Scan protocol and dose modulation. The maximum dose is delivered from 65% to 80% of the RR interval. In the remaining phases, the tube current drops to 4% of the dose. Within this modulation phase, reconstruction window position can be chosen (width 75 ms). *Abbreviations: ECG, electrocardiogram*

reconstructions based on the ECG signal were done on the angiography scans to obtain images free from motion artifacts in the maximum-dose time window (65-80% of the RR interval). The optimal diastolic phase was automatically obtained within this time window (Best-Phase, Siemens, Germany).

CT image reconstruction

For the study, additional reconstructions of the optimal diastolic phase were performer with the following parameters: effective slice thickness of 0.6 and 0.75 mm; reconstruction increment 0.4 mm; FOV 150-160 mm; three different standard convolution kernels (B26-B30-B46; FBP) and three comparable convolution kernel with first-generation iterative reconstruction (I26-I30-I46; IRIS, Siemens, Germany) (Figure 2).

CT image evaluation

The reconstructed images were transferred to a dedicated workstation with a cardiovascular software platform (SyngoVia, Siemens, Germany). To quantify the CT vascular attenuation value [expressed in Hounsfield units (HU)] and degree of attenuation obtained from the arrival of iodinated contrast material (enhancement), three regions of interest (ROIs) were placed in the ascending aorta (Ao), right (RCA) and left (LCA) coronary artery, respectively.

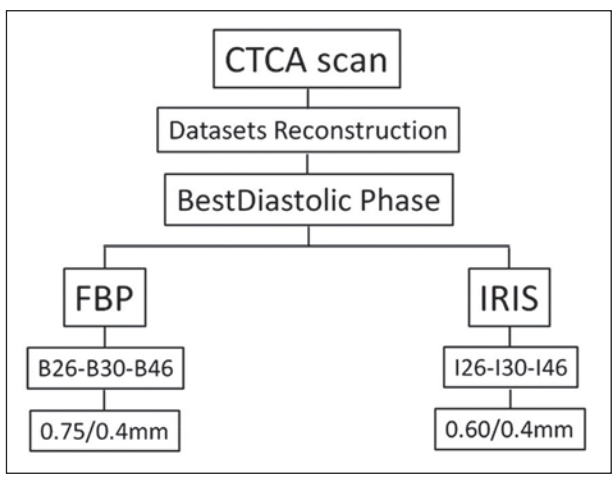

Figure 2. Study design. Immediately after CTCA scan, four datasets were reconstructed within BestDiastolic Phase using two different algorithms (i.e. FBP and IRIS) for both slice thickness of 0.75mm and 0.6mm.
Abbreviations: CTCA Scan, Computer Tomography Coronary Angiography; Series, kind of datasets; FBP, dataset reconstructed using FBP, the standard convolution kernel; IRIS, dataset reconstructed using IRIS, the iterative algorithm; B26-B30-B46, FBP reconstructions; I26-I30-I46, IRIS reconstructions; 0.75/0.4, slice thickness/increment; 0.6/0.4, slice thickness/increment

The SNR and CNR were calculated as follows:

$$SNR = \frac{\text{Vascular Density}}{\text{DS (air)}}$$

and

$$CNR = \frac{\text{Vascular Density} - \text{Muscle Density}}{\text{DS (air)}}$$

where
- vascular density represents the average CT attenuation values measured in Ao, RCA and LAD
- muscle density represents the CT attenuation measured into the lateral wall of the left ventricle.

Statistical analysis

Normal distribution was described as mean and standard deviation (SD). For data analysis we used commercially available software (MedCalc v9.2.1.0, Mariakerke, Belgium). Agreements between CT values, slice thickness and convolution kernels were explored using ANOVA test and Pearson's correlation coefficient. Differences were investigated with Student's T test (2 tails) for paired samples setting a significance p-value cutoff less than 0.05 ($p<0.05$).

Results

A total of 204 datasets, 102 obtained using FBP and 102 using IRIS shows the CT values measured on FBP and IRIS images for both slice thickness (Table 2). There was no significant difference between the CT attenuation values measured with different convolution kernels, except for the noise ($r=0.34$; $p<0.05$) (Figure 3). Comparing FBP vs. IRIS, CT value of Ao was 458 HU vs. 456 HU, RCA 448 HU vs. 446 HU,

Table 2. CT vascular attenuation values

	Measurement site							
	Ao	SD	RCA	SD	IVA	SD	SD_{air}	SD
FBP	458,26	75,04	448,40	93,56	444,40	97,27	24,04*	16,79
IRIS	456,17	76,00	445,55	101,86	442,00	76,61	18,83*	23,13

The Table 2 shows the CT vascular attenuation values (expressed in Hounsfield units - HU) measured in the ascending aorta (Ao), right (RCA) and left (LCA) coronary artery. The standard deviation in air was considered as the noise. We didn't find significant differences between the CT vascular attenuation values measured with different algorithms. Difference in noise was significant between FBP (24±SD) and IRIS (19±SD) (r=0.34; p<0.05). *p<0.05

Abbreviations: FBP, standard convolution kernel; IRIS, iterative algorithm reconstruction; Ao, ascending aorta; RCA, right coronary artery; LCA, left coronary artery; SD_{air}, standard deviation in air.

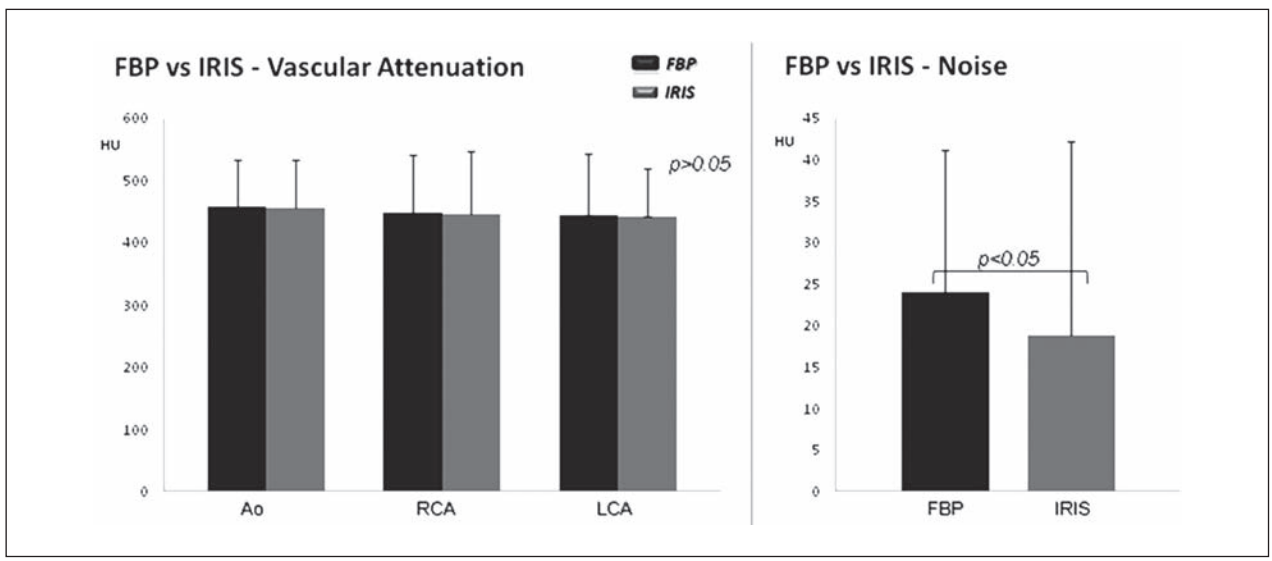

Figure 3. Attenuation values based on reconstruction algorithms.

Abbreviations: HU, Hounsfield Unit; FBP, standard convolution kernel; IRIS, iterative algorithm reconstruction; Ao, ascending aorta; RCA, right coronary artery; LAD, left coronary artery; Noise, standard deviation in air.

LCA 444 HU vs. 442 HU and Noise 24 vs. 19 HU (p<0.05 – Table 2). Lowest noise was found for IRIS using 0.6 mm (17HU – Table 3). Respect to image quality, we found a significant differences between FBP and IRIS, for both slice thickness (Table 4). IRIS can provide SNR and CNR significantly higher with increasing kernel sharpness (p<0.05 – Figure 4). SNR was 33.3±25.1, 77.3±51.7, 37.2±36.6, 64.4±59.2, while CNR was 25.32±19.8, 58.0±36.0, 28.6±23.5, 47.6±47.3 for 0.75B, 0.75I, 0.6B and 0.6I, respectively. IRIS showed an improved SNR of 57% and 56% for 0.75 mm and 0.6 mm, respectively, and an improved CNR of 42% and 40% (Figure 5).

Table 3. CT vascular attenuation values

	Measurement site			
Series	Ao	RCA	LCA	SD_{air}
0.75B	458,95	444,91	448,51	21,19
0.75I	457,87	438,66	439,41	20,59
0.60B	457,56	451,89	440,29	26,88
0.60I	454,48	452,44	444,59	17,08

Abbreviations: Series, kind of datasets; 0.75B and 0.6B, datasets reconstructed using FBP; 0.75I and 0.6I, datasets reconstructed using IRIS; Ao, ascending aorta; RCA, right coronary artery; LCA, left coronary artery; SD_{air}, standard deviation in air (Noise)

Table 4. SNR and CNR

	Slice Thickness					
	0.75 mm			0.60 mm		
	FBP	IRIS	p	FBP	IRIS	p
SNR	33.31	77.29	*p<0.05*	37.16	64.41	*p<0.05*
CNR	25.32	58.01	*p<0.05*	28.62	47.56	*p<0.05*

Abbreviations: SNR, signal-to-noise ratio; CNR, contrast-to-noise ratio; FBP, datasets reconstructed using standard convolution kernel; IRIS, dataset reconstructed using iterative algorithm

Discussion

We demonstrated a significant improvement in SNR and CNR by using first generation iterative reconstructions (IRIS) as compared to conventional FBP. Vascular attenuation of FBP and IRIS yielded similar values. The image noise (SD in air) was higher using FBP and both SNR and CNR were lower using FBP, as compared to IRIS. In particular, IRIS algo-

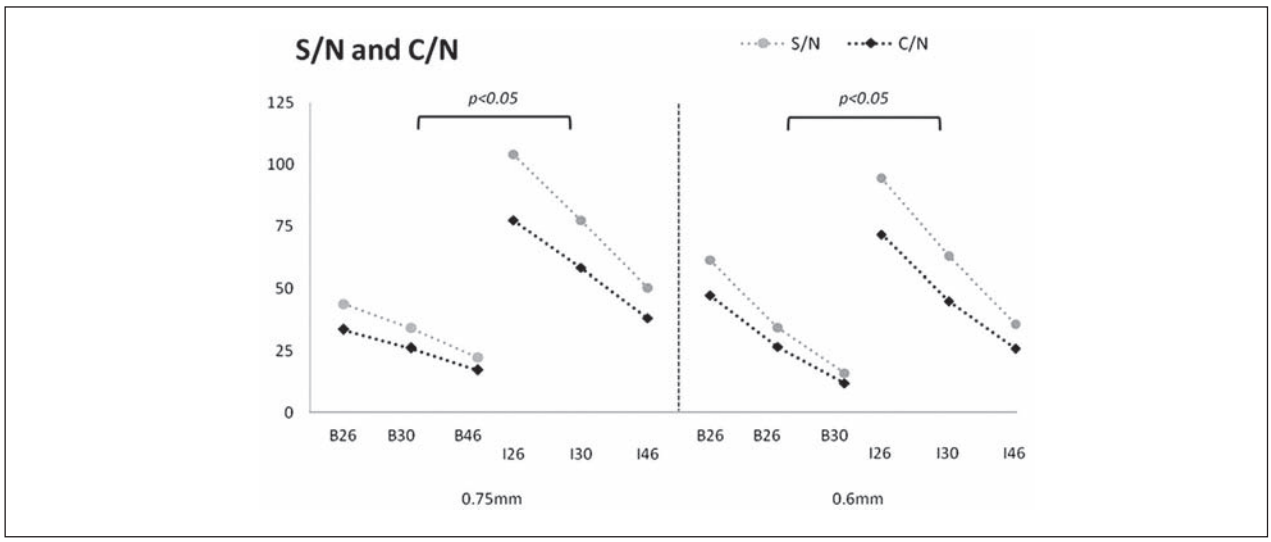

Figure 4. SNR and CNR based on different reconstruction algorithms.
Abbreviations: SNR, signal-to-noise ratio; CNR, contrast-to-noise ratio; 0.75mm and 0.6mm, datasets reconstructed using standard convolution kernel FBP (B26-B30-B46); 0.75mm and 0.6mm, datasets reconstructed using iterative algorithm (I26-I30-I46).

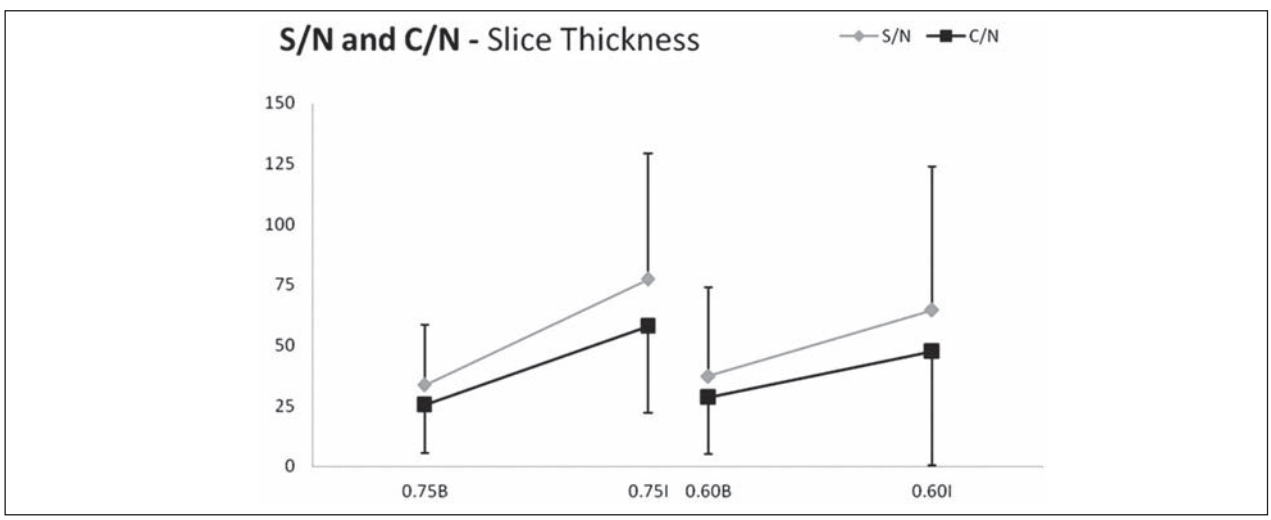

Figure 5. SNR and CNR based on different slice thickness.
Abbreviations: SNR, signal-to-noise ratio; CNR, contrast-to-noise ratio; 0.75B and 0.6B, datasets reconstructed using FBP; 0.75I and 0.6I, datasets reconstructed using IRIS

rithm further improved using a slice thickness slightly higher of the minimum collimation (i.e. 0.75 mm vs 0.6 mm) and with increasing of kernel sharpness.

Several previous non-coronary CT studies (30-32, 36, 37) demonstrated that use of iterative reconstruction algorithm, as compared with a standard FBP reconstruction algorithm, leads to lower the images noise and to significantly improved image quality and may allow further radiation reductions.

We hypothesized, that iterative reconstruction techniques would substantially lower quantum noise, enabling better evaluation of the vessel lumen, which have traditionally been recognized as limitation of cardiac CT.

Lower image noise with the IRIS reconstruction techniques allow the use of sharper or greater edge-enhancement kernels, which may have contributed to the improved both SNR and CNR and aided in the visualization of small structures not satisfactorily evaluable with the more noise-prone filtered back projection technique. Furthermore, previous coronary CT studies showed an increase in SNR and CNR; those studies concluded that iterative reconstruction techniques improves coronary imaging and may allow radiation dose reductions (38-40).

The finding of concomitant lower noise and higher SNR and CNR with better vessel sharpness using IRIS compared with FBP analysis may have an important clinical implication for the evaluation of coronary artery plaques that needs to be validated in vivo. Qualitative image analysis revealed higher mean luminal CT numbers on average in images reconstructed with IRIS than in those reconstructed with FBP.

Conclusion

In CTCA, iterative reconstruction provide a significantly lower noise and higher signal/noise compared with the conventionally used FBP (41-45). Thus, improved IRIS's image quality enables an increase in diagnostic confidence and/or a reduction in radiation dose.

References

1. Ferencik M, Chan RC, et al. Arterial wall imaging: evaluation with 16-section multidetector CT in blood vessel phantoms and ex vivo coronary arteries. Radiology 2006; 240 (3): 708-16.
2. Hoffmann U, Moselewski F, et al. Noninvasive assessment of plaque morphology and composition in culprit and stable lesions in acute coronary syndrome and stable lesions in stable angina by multi detector computed tomography. J Am Coll Cardiol 2006; 47 (8): 1655-62.
3. Hoffmann U, Nagurney JT, et al. Coronary multidetector computed tomography in the assessment of patients with acute chest pain. Circulation 2006; 114 (21): 2251-60.
4. Leber AW, Johnson T, et al. Diagnostic accuracy of dual-source multi-slice CT-coronary angiography in patients with an intermediate pretest likelihood for coronary artery disease. Eur Heart J 2007; 28 (19): 2354-60.
5. Leschka S, Alkadhi H, et al. Accuracy of MSCT coronary angiography with 64-slice technology: first experience. Eur Heart J 2005; 26 (15): 1482-7.
6. Leber AW, Knez A, et al. Quantification of obstructive and nonobstructive coronary lesions by 64-slice computed tomography: a comparative study with quantitative coronary angiography and intravascular ultrasound. J Am Coll Cardiol 2005; 46 (1): 147-54.
7. Leber AW, Knez A, et al. Accuracy of multidetector spiral computed tomography in identifying and differentiating the composition of coronary atherosclerotic plaques: a comparative study with intracoronary ultrasound. J Am Coll Cardiol 2004; 43 (7): 1241-7.
8. Schmermund D, Baumgart G, et al. Coronary artery calcium in acute coronary syndromes: a comparative study of electron-beam computed tomography, coronary angiography, and intracoronary ultrasound in survivors of acute myocardial infarction and unstable angina. Circulation 1997; 96 (5): 1461-9.
9. Knez A, Becker C, et al. Determination of coronary calcium with multi-slice spiral computed tomography: a comparative study with electron-beam CT. Int J Cardiovasc Imaging 2002; 18 (4): 295-303.
10. Leber AW, Becker A, et al. Accuracy of 64-slice computed tomography to classify and quantify plaque volumes in the proximal coronary system: a comparative study using intravascular ultrasound. J Am Coll Cardiol 2006; 47(3): 672-7.
11. Kopp AF, Schroeder S, et al. Non-invasive characterisation of coronary lesion morphology and composition by multislice CT: first results in comparison with intracoronary ultrasound. Eur Radiol 2001; 11:1607-11.
12. Schroeder S, Kopp AF, et al. Noninvasive detection and evaluation of atherosclerotic coronary plaques with multislice computed tomography. J Am Coll Cardiol 2001; 37: 1430-5.
13. Achenbach S, Moselewski F, et al. Detection of calcified and noncalcified coronary atherosclerotic plaque by contrast-enhanced, submillimeter multidetector spiral computed tomography: a segment-based comparison with intravascular ultrasound. Circulation 2004; 109: 14-7.
14. Leber AW, Knez A, et al. Accuracy of multidetector spiral computed tomography in identifying and differentiat-

ing the composition of coronary atherosclerotic plaques: a comparative study with intracoronary ultrasound. J Am Coll Cardiol 2004; 43: 1241-7.
15. Leber AW, Becker A, et al. Accuracy of 64-slice computed tomography to classify and quantify plaque volumes in the proximal coronary system a comparative study using intravascular ultrasound. J Am Coll Cardiol 2006; 47: 672-7.
16. Leber AW, Knez A, et al. Quantification of obstructive and nonobstructive coronary lesions by 64-slice computed tomography a comparative study with quantitative coronary angiography and intravascular ultrasound. J Am Coll Cardiol 2005; 46: 147-54.
17. Leber AW, Knez A, et al. Composition of coronary atherosclerotic plaques in patients with acute myocardial infarction and stable angina pectoris determined by contrast-enhanced multislice computed tomography. Am J Cardiol 2003; 91: 714-8.
18. Budoff MJ, Cohen MC, et al. ACCF/AHA clinical competence statement on cardiac imaging with computed tomography and magnetic resonance: a report of the American College of Cardiology Foundation/American Heart Association/American College of Physicians Task Force on Clinical Competence and Training. J Am Coll Cardiol 2005; 46: 383-402.
19. Becker CR, Nikolaou K, et al. Ex vivo coronary atherosclerotic plaque characterization with multi-detector-row CT. Eur Radiol 2003; 13: 2094-8.
20. Schroeder S, Flohr T, et al. Accuracy of density measurements within plaques located in artificial coronary arteries by X-ray multislice CT: results of a phantom study. J ComputAssist Tomogr 2001; 25: 900-6.
21. Cademartiri F, Mollet NR, et al. Influence of intracoronary attenuation on coronary plaque measurements using multislice computed tomography: observations in an ex vivo model of coronary computed tomography angiography. Eur Radiol 2005; 15: 1426-31.
22. Flohr TG, McCollough CH, et al. First performance evaluation of a dual-source CT (DSCT) system. Eur Radiol 2006; 16: 256-68.
23. Johnson TR, Nikolaou K, et al. Dual-source CT cardiac imaging: initial experience. Eur Radiol 2006; 16: 1409-15.
24. Suzuki S, Furui S, et al. Measurement of vascular diameter in vitro by automated software for CT angiography: effects of inner diameter, density of contrast medium, and convolution kernel. AJR Am J Roentgenol 2004; 182: 1313-7.
25. Seifarth H, Raupach R, et al. Assessment of coronary artery stents using 16-slice MDCT angiography: evaluation of a dedicated reconstruction kernel and a noise reduction filter. Eur Radiol 2005; 15: 721-6.
26. Hara AK, Paden RG, et al. Iterative reconstruction technique for reducing body radiation dose at CT: feasibility study. AJR 2009; 193: 764-71.
27. Prakash P, Kalra MK, et al. Diffuse lung disease: CT of the chest with adaptive statistical iterative reconstruction technique. Radiology 2010; 256 (1); 261-9.
28. Marin D, Nelson RC, et al. Low-tube-voltage, high-tube-current multidetector abdominal CT: improved image quality and decreased radiation dose with adaptive statistical iterative reconstruction algorithm – initial clinical experience. Radiology 2010; 254 (1): 145-53.
29. Prakash P, Kalra MK, et al. Reducing abdominal CT radiation dose with adaptive statistical iterative reconstruction technique. Invest Radiol 2010; 45 (4): 202-10.
30. Nuyts J, De Man B, et al. Iterative reconstruction for helical CT: a simulation study. Phys Med Biol 1998; 43: 729-37.
31. Liu YJ, Zhu PP, et al. A new iterative algorithm to reconstruct the refractive index. Phys Med Biol 2007; 52: L5-L13.
32. Cheng LC, Fang T, et al. Fast iterative adaptive reconstruction in low-dose CT imaging. Los Alamitos CA IEEE; 2006; 889-92.
33. Cademartiri F, Malagutti P, et al. Non-invasive coronary angiography with 64-slice computed tomography. Minerva Cardioangiol 2005; 53: 465-72.
34. Cademartiri F, Runza G, et al. Introduction to coronary imaging with 64-slice computed tomography. Radiol Med 2005; 110: 16-41.
35. Maffei E, Martini C, et al. Low dose CT of the heart: a quantum leap into a new era of cardiovascular imaging. Radiol Med 2010; 115: 1179-207.
36. Yanagawa M, Honda O, et al. Adaptive statistical iterative reconstruction technique for pulmonary CT: image quality of the cadaveric lung on standard- and reduced-dose CT. Acad Radiol 2010; 17 (10): 1259-66.
37. Prakash P, Kalra MK, et al. Radiation dose reduction with chest computed tomography using adaptive statistical iterative reconstruction technique: initial experience. J Comput Assist Tomogr 2010; 34 (1): 40-5.
38. Tricarico F, Hlavacek AM, et al. Cardiovascular CT angiography in neonates and children: Image quality and potential for radiation dose reduction with iterative image reconstruction techniques. Eur Radiol 2012 Dec 4. [Epub ahead of print]
39. Moscariello A, Takx RA, et al. Coronary CT angiography: image quality, diagnostic accuracy, and potential for radiation dose reduction using a novel iterative image reconstruction technique-comparison with traditional filtered back projection. Eur Radiol 2011; 21 (10): 2130-8.
40. Ebersberger U, Tricarico F, et al. CT evaluation of coronary artery stents with iterative image reconstruction: improvements in image quality and potential for radiation dose reduction. Eur Radiol 2013; 23 (1): 125-32.
41. Funabashi N, Irie R, Aiba M, Morimoto R, Kabashima T, Fujii S, Uehara M, Ozawa K, Takaoka H, Kobayashi Y. Adaptive-Iterative-Dose-Reduction 3D with multi-sector-reconstruction method in 320-slice CT may maintain accurate-measurement of the Agatston-calcium-score of severe-calcification even at higher pulsating-beats and low tube-current in vitro. Int J Cardiol 2013 Feb 25. doi:pii: S0167-5273(13)00290-8. 10.1016/j.ijcard.2013.01.230 [Epub ahead of print].
42. Gebhard C, Fiechter M, Fuchs TA, Ghadri JR, Herzog BA,

Kuhn F, Stehli J, Müller E, Kazakauskaite E, Gaemperli O, Kaufmann PA. Coronary artery calcium scoring: Influence of adaptive statistical iterative reconstruction using 64-MDCT. Int J Cardiol 2012 Sep 5. [Epub ahead of print].

43. Guaricci AI, Maffei E, Brunetti ND, Montrone D, Di Biase L, Tedeschi C, Gentile G, Macarini L, Midiri M, Cademartiri F, Di Biase M. Heart rate control with oral ivabradine in computed tomography coronary angiography: A randomized comparison of 7.5mg vs 5mg regimen. Int J Cardiol 2012 Oct 9. doi: pii: S0167-5273(12)01147-3. 10.1016/j.ijcard.2012.09.041. [Epub ahead of print]
44. Guaricci AI, Schuijf JD, Cademartiri F, Brunetti ND, Montrone D, Maffei E, Tedeschi C, Ieva R, Di Biase L, Midiri M, Macarini L, Di Biase M. Incremental value and safety of oral ivabradine for heart rate reduction in computed tomography coronary angiography. Int J Cardiol 2012; 156 (1): 28-33.
45. Di Tanna GL, Berti E, Stivanello E, Cademartiri F, Achenbach S, Camerlingo MD, Grilli R.Informative value of clinical research on multislice computed tomography in the diagnosis of coronary artery disease: A systematic review. Int J Cardiol 2008; 130 (3): 386-404.

Received: 24 March 2014
Accepetd: 29 August 2014
Correspondance:
Prof. Dr. Filippo Cademartiri, MD, PhD, FESC, FSCCT
Cardio-Vascular Imaging Unit - Giovanni XXIII Clinic
Via Giovanni XXIII, 7
31050 Monastier di Treviso (TV), Italy
Tel. +39 0422 896710
Fax +39 0422 896507
E-mail: filippocademartiri@gmail.com